


Article

# Study on Well Selection Method for Refracturing Horizontal Wells in Tight Reservoirs

Qihong Feng<sup>1</sup>, Jiawei Ren<sup>1</sup>, Xianmin Zhang<sup>1,\*</sup>, Xianjun Wang<sup>2</sup>, Sen Wang<sup>1</sup>  and Yurun Li<sup>1</sup>

<sup>1</sup> School of Petroleum Engineering, China University of Petroleum (East China), Qingdao 266580, China; fengqihong.upc@gmail.com (Q.F.); rjwupc@163.com (J.R.); fwforest@gmail.com (S.W.); 1404020204@s.upc.edu.cn (Y.L.)

<sup>2</sup> Daqing Oilfield Company Limited Production Technology Institute, Daqing 163000, China; wangxianjun@petrochina.com.cn

\* Correspondence: Spemin@126.com; Tel.: +86-185-6390-5501

Received: 19 July 2020; Accepted: 11 August 2020; Published: 14 August 2020



**Abstract:** Refracturing technology is one of the key technologies to recover the productivity of horizontal wells in tight oil reservoirs, and the selection of best candidate wells from target blocks is the basis of this technology. Based on the refracturing production database, this paper analyzes the direct relationship between geological data, initial fracturing completion data, and dynamic production data, and the stimulation effect of refracturing. Considering the interaction among multiple factors, the factors affecting the stimulation effect of refracturing are classified and integrated, and a comprehensive index including geology, engineering, and production is constructed, making this index meaningful both for physical and engineering properties. The XGBoost decision tree model is established to analyze the weight of influence for the comprehensive index of geology, engineering, and production in predicting the stimulation effect of refracturing. A comprehensive decision index of refracturing well selection is formed by combining the above three for performing a fast selection of horizontal candidate wells for fracturing. Taking a horizontal well test area in Songliao Basin as an example, the target wells of refracturing are selected by this method, and field operation is carried out, and a good stimulation effect is achieved. The results show that the comprehensive decision-making index constructed by this method is reliable and has certain guiding significance for well selection and stimulation potential evaluation of tight oil reservoir.

**Keywords:** tight oil; re-fracturing; horizontal wells; decision index; XGBoost regression; deep learning

## 1. Introduction

Tight oil is a key component of unconventional oil and gas resources and has great potential for exploitation [1]. Volume fracturing has become the core technology to develop tight oil and gas reservoirs [2–4]. However, with the development of depletion development, the decline of formation pressure causes fracture closure failure, resulting in a rapid decline of production and low recovery of a single well. At the same time, due to an unclear understanding of the reservoir or limited by fracturing technology and equipment, the production of some horizontal wells will drop sharply after fracturing, and the initial stimulation measures will fail. Refracturing technology is an effective way to recover or increase single well production and prolong the stable production cycle [5–7].

The primary problem of refracturing technology is how to screen out the horizontal wells with the greatest stimulation potential from several low production horizontal wells in the target block. Many scholars have done a lot of work on well selection for refracturing. Roussel and Sharma [8], and Sinha and Ramakrishnan [9] selected the candidate wells for refracturing through the processing of historical production data, but the geological factors and the degree of completion of primary

fracturing were not considered in this method. Tavasoli [10] used the numerical simulation method to simulate the refracturing productivity of several fractured horizontal wells so as to select the candidate wells. The result of well selection was highly reliable, but the workload of reservoir modeling and history fitting was heavy, and the well selection efficiency was low. Oberwinkler and Economides [11], and Saeedi et al. [12] used an artificial neural network for machine learning. The calculation speed is fast, and the accuracy is high. However, due to the limited number of field sample library and the limitation of algorithm structure, it is easy to overfit and lead to poor generalization [13]. Zeng [14] combined the fuzzy comprehensive evaluation method with the grey correlation theory, which has rich well selection indexes. However, the fuzzy evaluation relies too much on experience, and the subjective factors have great influence. In addition, a large number of well selection methods are carried out for fractured vertical wells, and the formed methods are no longer applicable to fractured horizontal wells [15,16].

To sum up, there are many factors that affect the well selection decision-making of refracturing, and an efficient and quantitative well selection method for fractured horizontal wells is needed in the mine. Based on a tight reservoir as the research object, this paper establishes the simulation model of refracturing, carries out a large number of numerical simulation, and establishes the refracturing production database, and then analyzes the relationship between geological data, completion data of primary fracturing and dynamic production data and the stimulation effect of refracturing. Considering the interaction among multiple factors, the stimulation effect of refracturing will be affected by the comprehensive index geology, engineering, and production and is constructed by the combination of various factors. The deep learning method can strengthen the feature learning trained on big data samples, and can mine rich and comprehensive information. Through the establishment of the XGBoost decision tree model, the influence weight of geological, engineering, and production, a comprehensive index in predicting the stimulation effect of refracturing is analyzed. Finally, the above three kinds of comprehensive indexes are combined to form the comprehensive decision index of refracturing well selection. The rapid well selection decision for refracturing horizontal wells in tight oil reservoirs is presented.

## 2. Establishing a Refracturing Production Database

A large-scale refracturing test has not been carried out in the target oilfield, and the refracturing production wells are limited, so it is impossible to make a large number of statistics on the relationship between the increase in oil after refracturing and the influencing factors. In view of this, based on the actual situation of the target reservoir, a numerical simulator (CMG) was used to establish a series of geological models. The plane size of the model was 2000 m × 800 m, and the permeability of 300 groups of horizontal wells with average permeability of 0.05 mD to 1.2 mD was generated by sequential Gaussian generator (Figure 1). The porosity was assigned according to the pore permeability fitting relationship of Daqing tight oil reservoir. The model set up a horizontal single well, prefabricated the artificial fracture of the initial fracturing, fixed the bottom hole flow pressure production for 5 years, on this basis of extracting pressure and saturation fields, set the artificial fracture of refracturing again, and opened the well again for 5 years. The fracture parameters, such as half-length, fracture width, and conductivity, were introduced into the reservoir numerical model by using the fracturing design software according to the actual operation conditions of the oilfield. The fracturing operation parameters, such as fracturing fluid dosage and sand addition, were equivalent to the fracture parameters, such as fracture half-length and conductivity. Other parameters, such as reservoir depth, thickness, initial pressure, and production pressure difference, were simulated by using the algorithm to generate a random parameter combination scheme according to the actual situation of the reservoir (Figure 2). The geological parameters, fracture parameters, production parameters after the initial fracturing and corresponding refracturing oil increment of each simulation scheme were collected, and the actual data of refractured production wells in the field were integrated to form a refracturing Production database. A total of 289 sets of digital simulation scheme samples, and 5 groups of actual

data samples were collected. The minimum value of refracturing oil increment in the sample set was 1719 t, the maximum value was 15,035 t, and the average value was 6456.4 t. In view of the accuracy of statistical data and the error of numerical simulation, there will be some noise data in the data set. According to the actual experience, outlier data was eliminated and replaced, and finally, collected. Two hundred and fifty-eight sets of sample data were used to establish the refracturing production database. Part of the sample database data can be seen in Appendix A.

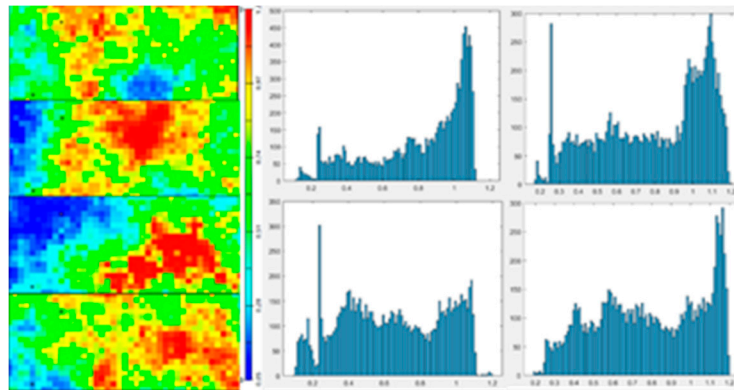


**Figure 1.** Reservoir numerical simulation model partial permeability image and its distribution.

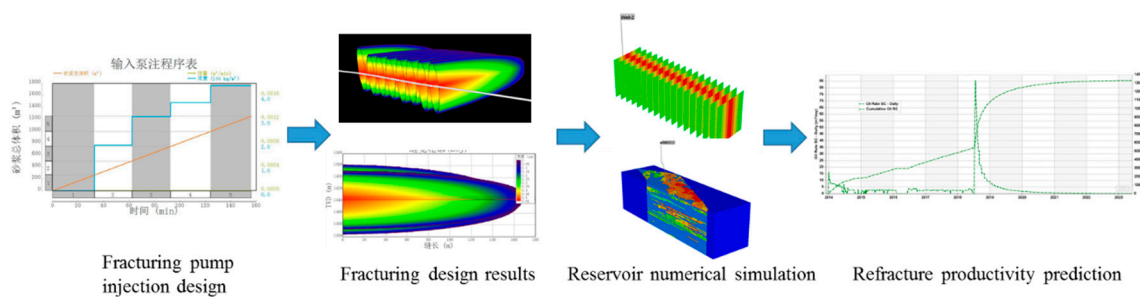


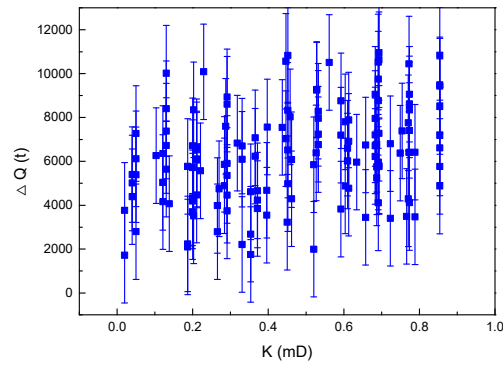
**Figure 2.** Workflow for predicting refracturing oil increase.

### 3. Construction of the Comprehensive Evaluation Index

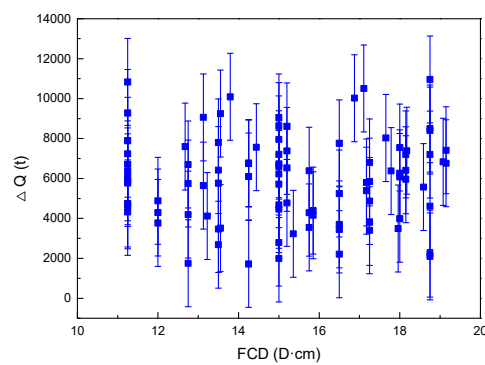
The success of refracturing is related to reservoir physical properties, initial fracturing operation, and production performance. Therefore, on the premise of ensuring the collectability and comprehensiveness of indexes, the factors influencing the refracturing effect were summarized and screened. Permeability, porosity, reservoir thickness, and reservoir pressure parameters to represent the geological characteristics of the candidate well were selected. The selection of parameters, such as fracturing fluid consumption, fracturing sand addition, number of fracturing clusters, footage of horizontal well, drilling rate of oil-bearing sandstone, were added to characterize the initial fracturing and the current effective status of hydraulic fractures. By selecting parameters, such as cumulative oil production, cumulative fluid production, fracturing fluid flow back volume, initial production, average production, bottom hole flow pressure, the productivity changes in candidate wells after initial fracturing were characterized.

This paper analyzes and compares the relationship between the increment of refracturing oil and the geological parameters, such as permeability, the engineering parameters, such as fracture half-length, and the production parameters, such as bottom hole flow pressure of each production well in the refracturing database, (Figure 3). From the analysis results of influencing factors, it can be concluded that although there is a certain relationship between the stimulation effect of refracturing and geological, completion, dynamic production, and other factors, the single factor or several factors are not obvious, and the overall performance is relatively scattered. At the same time, the influencing factors are not independent, so it is difficult to quantitatively characterize the effect of refracturing

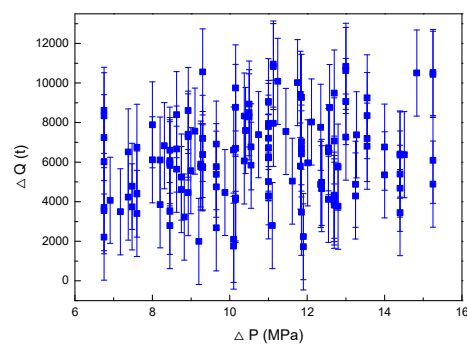
through a few simple parameters. However, there should more or less be a mapping relationship between the influencing factors. Therefore, considering the interaction between multiple factors, the factors that affect the effect of refracturing were classified and integrated to make them meaningful both for physical and engineering properties.



(a)



(b)



(c)

**Figure 3.** Relationship between refracturing oil increase and single factor: (a) Production increase versus permeability; (b) Production increase versus Fracture conductivity; (c) Production increase versus production pressure difference.

### 3.1. Geological Composite Index $G_i$

For reservoir characteristics, such as reservoir thickness, porosity, permeability, oil saturation, and other physical parameters, the higher the value, the higher the recoverable reserves of the reservoir, the greater the stimulation potential of refracturing. At the same time, the footage of horizontal well is directly related to the contact area of the reservoir. Therefore, the reservoir porosity, permeability, effective thickness, and the length of oil-bearing sandstone drilled in horizontal wells, are positively correlated with the stimulation potential after refracturing. However, from the single factor influence rule diagram, the overall performance was relatively scattered. To explore the impact of the overall geological factors on the impact of refracturing oil production, the geological influence factors were multiplied to represent the comprehensive geological index, so as to characterize the geological stimulation potential of horizontal well refracturing. The higher the value, the greater the stimulation potential of refracturing. To remove the scale-unit dependency of variables, each variable was normalized into a dimensionless quantity, which was more convenient for comparison and weighted analysis of different categories or orders of magnitude indicators. The expression and normalized calculation methods are as follows. Based on the refracturing production database, calculate and count the geological comprehensive index of each horizontal well and the cumulative oil production increase in five years after refracturing, and draw the relationship between the geological comprehensive index and the increase in fracturing oil (Figure 4).

$$\begin{cases} G = L \times D_r \times K \times \phi \times h_e \\ G_I = \frac{G}{G_{\max}} \end{cases} \quad (1)$$

where  $L$  is the footage of horizontal well;  $D_r$  is the drilling rate of oil-bearing sandstone;  $K$  is the permeability of the candidate well reservoir, mD;  $\phi$  is the porosity of the candidate well reservoir;  $h_e$  is the average effective thickness of the candidate well reservoir, m;  $S_o$  is the oil saturation of the candidate well reservoir.

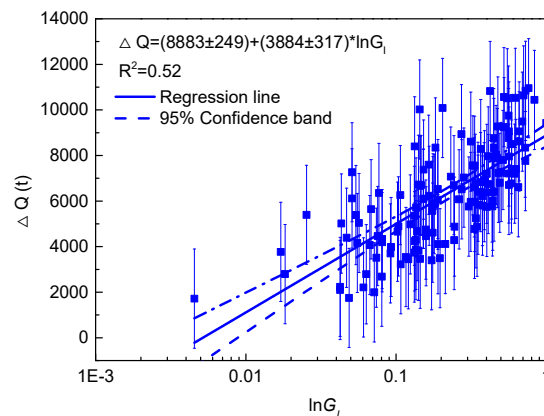


Figure 4. Production increase versus Geological composite index.

### 3.2. Engineering Composite Index $E_I$

On the premise of good reservoir and production conditions, the larger the scale of the initial fracturing, such as more fracturing sections, the larger amount of fracturing fluid and sand, the reservoir development degree within the effective period of fracturing production had reached a higher level. At this time, it is difficult to obtain considerable production and investment return by refracturing this kind of oil well. Therefore, a reservoir with a low degree of primary fracturing should be selected as far as possible for secondary stimulation during refracturing, considering the degree of primary fracturing per unit length of horizontal wells. The engineering comprehensive index  $E_I$  is defined to characterize the degree of primary fracturing in horizontal wells, the higher the value, represents

the greater the degree of initial fracturing reconstruction per unit length of a horizontal well, the smaller the stimulation potential of refracturing. The expression and normalized calculation methods are as follows. Based on the refracturing production database, calculate and count the engineering comprehensive index of each horizontal well and the cumulative oil production increase in five years after refracturing, and draw the relationship between the engineering comprehensive index and the increase in fracturing oil (Figure 5).

$$\begin{cases} E = \frac{V_s \times SP \times N}{L \times D_r} \\ E_I = \frac{E}{E_{\max}} \end{cases} \quad (2)$$

where  $V_s$  is the total amount of fracturing fluid used in the initial fracturing process,  $m^3$ ;  $SP$  is the fracturing fluid sand ratio;  $N$  is the total fracture cluster number of horizontal wells.

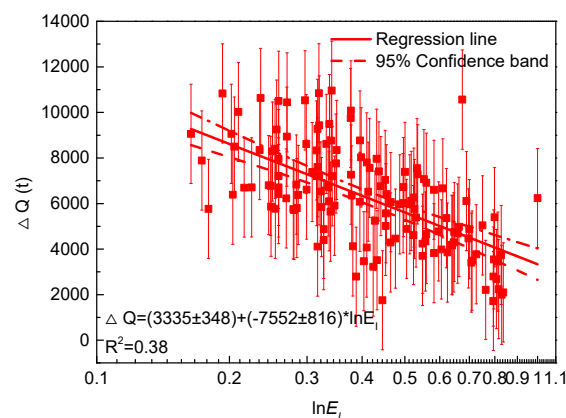


Figure 5. Production increase versus Engineering composite index.

### 3.3. Production Composite Index $P_I$

Reese et al. [17] and Popa et al. [18] proposed that the wells with higher productivity after initial fracturing will also have high yield after refracturing. Therefore, the selection of candidate wells for refracturing should be focused on the high-yield wells after primary fracturing. It can be considered that the production performance after the first fracturing is also related to the stimulation potential after refracturing. The production pressure difference of production well reflects the liquid production capacity and formation pressure maintaining level. The initial fracturing fluid flow back also affects the production level of oil wells. The difference between the cumulative fluid production and the flow back rate is the amount of fracturing fluid storage fluid, which can maintain and supplement the formation energy to a certain extent. However, the reservoir damage caused by the formation retained by the fracturing fluid count cannot be ignored. If the fracturing fluid count does not flow back in time, the effective seepage area will be reduced, and the fracturing effect will be weakened [19]. The fracturing fluid flow back rate of tight oil wells in the target test area is usually maintained at 10–50%. Therefore, the ratio  $A$  of production pressure difference to fracturing storage fluid volume was constructed. The larger the value, the greater the production pressure difference, or the smaller the amount of reservoir fluid, the greater the potential for production increase after refracturing.

$$A = \frac{P_i - P_w}{N_l - N_s} \quad (3)$$

where  $P_i$  is the original formation pressure, MPa;  $P_w$  is the bottom hole flowing pressure, MPa;  $N_l$  is the accumulated liquid production of horizontal wells, t;  $N_s$  is the fracturing fluid return flow rate, t.

The productivity decline of horizontal wells can also represent the relevant characteristics of tight reservoirs. The higher the initial production after fracturing, the greater the short-term fracture conductivity and the stronger fluid supply capacity of the reservoir. The average daily production during the production period indicates the average oil production capacity of the reservoir up to the present. The difference between the initial production after fracturing and the average daily production in the production period is defined as the degree of production decline. The larger the value, the more serious the production decline after the first fracturing. At the same time, horizontal wells in tight reservoirs need to ensure a certain amount of cumulative oil production to ensure effective investment recovery [20]. Therefore, the ratio  $B$  of the difference between the initial production and the average daily production and the cumulative oil production. A larger dimensionless ratio  $B$  indicates that the production declines seriously at the first fracturing or that the cumulative oil production and the repeated production potential is greater.

$$B = \frac{C_{ob} - C_{oa}}{N_o} \quad (4)$$

where  $N_s$  is the fracturing fluid return flow rate, t;  $C_{ob}$  is the monthly production in the initial stage of fracturing, t/month;  $C_{oa}$  is the average monthly production, t/month;  $N_o$  is the cumulative oil production of horizontal wells, t.

The production factor  $P_i$  is defined as the product of the combination dimensionless index  $A$  and  $B$ . The greater the  $P_i$ , the higher the oil production potential of the target horizontal well is, and the lower the recovery degree after the initial fracturing production, the greater the stimulation potential of the target well after refracturing. Based on the refracturing production database, calculate and count the production comprehensive index of each horizontal well and the cumulative oil production increase in five years after refracturing, and draw the relationship between the production comprehensive index and the increase in fracturing oil (Figure 6).

$$\begin{cases} P = A \times B = \frac{P_i - P_w}{N_l - N_s} \frac{C_{ob} - C_{oa}}{N_o} \\ P_i = \frac{P}{P_{\max}} \end{cases} \quad (5)$$

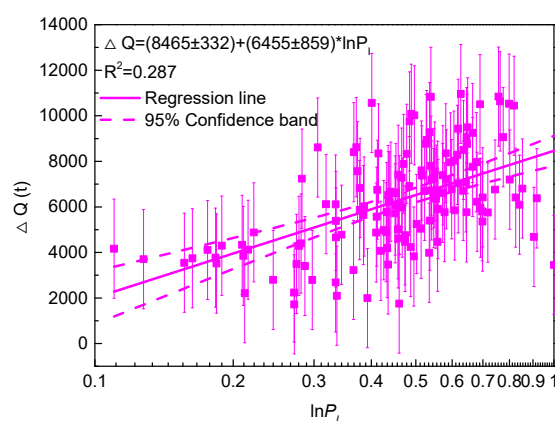


Figure 6. Production increase versus Production composite index.

#### 4. Construction of Comprehensive Decision Index

Because the stimulation effect of refracturing is affected by many factors, such as geology, engineering, and production, it is necessary to determine the influence weight of the comprehensive index of geology, engineering, and production in predicting the stimulation effect of refracturing before establishing the comprehensive decision index. Conventional weight calculation methods, such as

analytic hierarchy process (AHP), surface response techniques (RSM), and grey correlation, all need the input of SME (subject matter expert) or design experiments in advance, which is too subjective and has no advantage in big data processing [14,21–23]. Deep learning methods in the field of artificial intelligence highlight the importance of feature learning [24–26]. Taking the decision tree model as an example, the depth and number of decision trees can be adjusted, and the number of hidden layers can be increased to make classification or prediction easier. Given massive data, it can extract rich and comprehensive effective information, and then use them to classify and predict. At the same time, it can accurately get the weight of each influencing factor, so as to reflect the actual problems in a more real way [27,28].

#### 4.1. Xgboost Decision Tree Modeling

XGBoost is a kind of lifting tree model, which belongs to a boosting algorithm. Its core idea is to form a strong classifier from multiple weak classifiers; that is, many tree models are integrated together to avoid the overfitting problem of tree models effectively. It has obvious advantages in regression accuracy [29,30], and the model expression is as follows:

$$\hat{y}_i = \sum_{k=1}^K f_k(x_i) \quad (6)$$

where  $f_k$  is the  $k$ th tree model;  $y_i$  is the prediction result of sample  $x_i$ , and the objective function of learning process loss is set as follows:

$$Obj^{(t)} = \sum_{i=1}^n l(y_i, \hat{y}_i^{(t-1)} + f_t(x_i)) + \Omega(f_t) + \text{const} \tan t \quad (7)$$

where  $l$  is the loss function, which satisfies the second-order differentiability, and  $\Omega(f_t)$  is the regularization term. Its specific form is

$$\Omega(f) = \gamma T + \frac{1}{2} \lambda \|\omega\|^2 \quad (8)$$

where  $T$  is the number of leaf nodes of the decision tree;  $\omega$  is the weight of each decision leaf node.

The objective function is obtained by Taylor second-order expansion of Formula (7)

$$\begin{cases} Obj^{(t)} \approx \sum_{i=1}^n l(y_i, \hat{y}_i^{(t-1)} + g_i f_t(x_i) + \frac{1}{2} h_i f_t^2(x_i)) + \Omega(f_t) + \text{const} \tan t \\ g_i = \delta_{\hat{y}_i^{(t-1)}} l(y_i, \hat{y}_i^{(t-1)}) \\ h_i = \delta^2_{\hat{y}_i^{(t-1)}} l(y_i, \hat{y}_i^{(t-1)}) \end{cases} \quad (9)$$

where  $g_i$  and  $h_i$  are the first and second derivatives of loss function  $l$  at  $y^{(t-1)}$ . To avoid overfitting in the training process, the algorithm does not train all regression trees at the same time but adds decision trees in turn. Therefore, when adding  $t$  trees, the previous  $t - 1$  tree has been trained; therefore,  $l(y_i, \hat{y}_i^{(t-1)})$  can be regarded as constant neglect, and the final objective function is simplified as follows:

$$Obj^{(t)} \approx \sum_{i=1}^n \left( g_i f_t(x_i) + \frac{1}{2} h_i f_t^2(x_i) \right) + \Omega(f_t) + \text{const} \tan t \quad (10)$$

After the decision tree model is created, the importance score can be obtained by calculating the improved performance measurement of each attribute in the dataset. The importance score measures the value of features in the construction of the promotion decision tree in the model. When an input parameter is used to build a decision tree in the model many times, the more important the parameter is.



#### 4.2. Algorithm Training and Prediction

Based on the refracturing production database, the comprehensive index of geology, engineering, and production of each horizontal well was calculated. The geological, engineering, and production indexes were taken as the input items, and the oil increment of refracturing was taken as the output item. During the training process, 90% of the learning sample data was used for training, verifying, and testing the model, and the remaining 10% of the data was used to predict the model after training. The XGBoost algorithm was optimized. Because the optimization of XGBoost regression algorithm involves the combination of multiple algorithm parameters, while the conventional grid search optimization method relies on traversing all parameters for optimization, so the workload is huge. Therefore, the strategy of adjusting parameters step by step was used to optimize the algorithm, and the optimal combination of algorithm parameters was finally found. The specific optimization steps are as follows.

(1) According to the conventional experience, a group of initial parameters was selected, and the number of decision trees was set as 50. On this basis, the maximum depth and minimum child weight were adjusted. The maximum depth and minimum child weight determine the complexity of the decision tree. The optimal combination of tree parameters can be found by drawing a heat map of the loss function with maximum depth and minimum child weight.

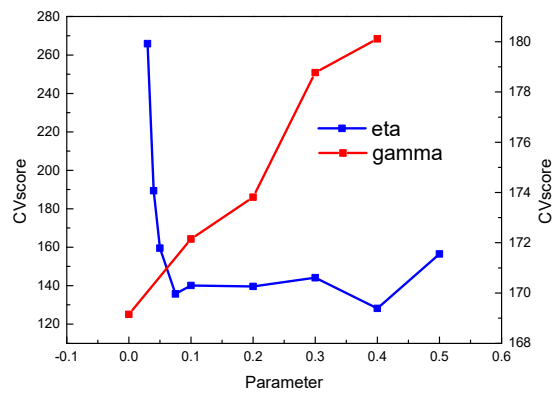
(2) Adjust the gamma; the parameter determines when the loss function is split, and the smaller the parameter is, the smaller the risk of overfitting is. Therefore, under the premise of ensuring the rationality of the loss function, gamma should be taken to be as small as possible.

(3) Adjust sample sampling mode; the parameters mainly involve colsample bytree and subsample. In the same way, the best parameter combination can be found by drawing a heat map of the loss function with two parameters.

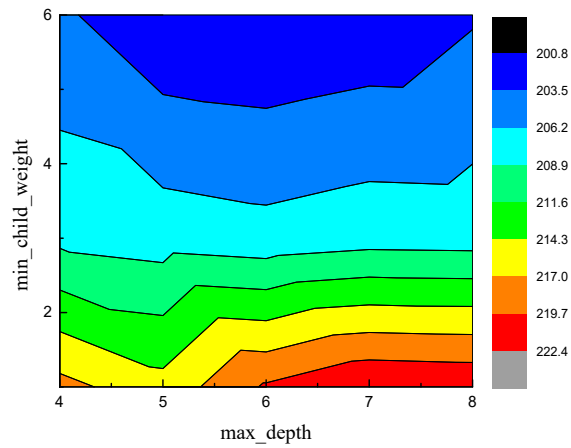
(4) Adjust the learning rate eta, compare the loss function to complete the eta parameter optimization.

Finally, the maximum depth was 8, the minimum child weight was 6, the colsample bytree was 0.8, the subsample was 0.6, and the learning rate (eta) was 0.4. The change in damage function with parameters in the optimization process is shown in Figure 7. Next, the correlation coefficient (Figure 8) between predicted oil increase and actual oil increase in the test set was calculated, in which abscissa was the actual oil increase in the production database, and the ordinate was the predicted value. The results showed that the intersection of the real value and the predicted value was near the 45° line. The correlation coefficient  $R^2$  between the predicted results and the real values was 0.9537. It can be concluded that the prediction error of XGBoost algorithm is small, and it has good generalization for samples without learning and training and can be weighted and analyzed to get the weight calculation results (Figure 9).

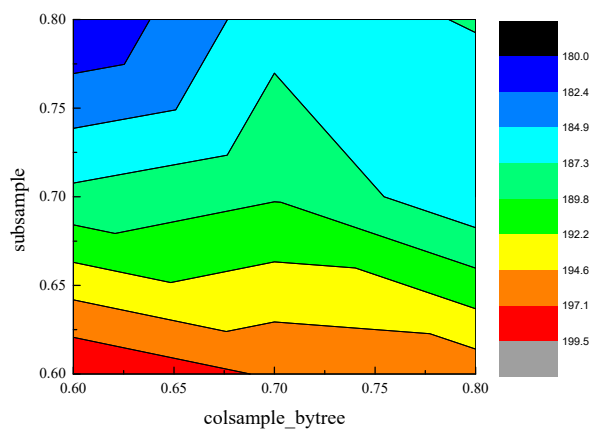
According to the weight calculation results, the weight coefficient of the engineering comprehensive index was the largest, up to 0.42, meaning that the completion of the initial fracturing was the main control factor of the refracturing effect. The weight coefficient of the production comprehensive index was 0.33, which indicates that the productivity situation in the production period after the end of the initial fracturing also had a great impact on the stimulation effect after refracturing, so the selection of candidate wells should be focused on the production performance after the initial fracturing. For the fracturing technology, the productivity contribution mainly depended on the fracture and its SRV, so the weight coefficient of the Geological comprehensive index was the smallest, reaching 0.25.



(a)



(b)



(c)

**Figure 7.** XGBOOST regression algorithm to optimize the parameter adjustment process: (a) eta and gamma parameter optimization; (b) max\_depth and min\_child\_weight parameter optimization; (c) colsample\_bytree and subsample parameter optimization.

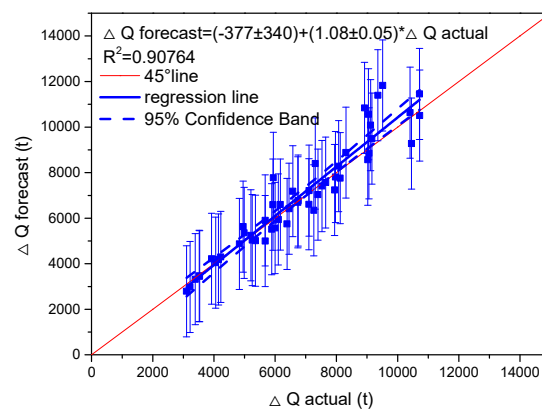


Figure 8. Intersection diagram of simulation data and verification data.

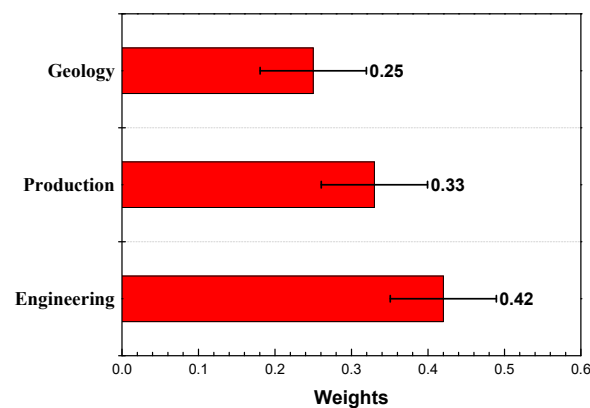


Figure 9. XGBoost output feature parameter weights.

#### 4.3. Comprehensive Decision Index $S_i$

Based on the weight calculation results, the comprehensive decision index  $S_i$  is defined as the weighted average of the comprehensive index of geology, engineering, and production, which was used to characterize the stimulation potential of a single well in all candidate wells. According to Figure 5, the greater the  $E_I$ , the lower the potential for refracturing; therefore, the  $\beta$  coefficient was negative. The formula can be used to sort all horizontal wells in a block according to the well selection index  $S_I$ , so as to screen out the horizontal wells with the greatest potential of refracturing production in the target block. The weight coefficients of each parameter were calculated by XGBoost classification prediction model, and the expression is as follows:

$$S_I = \alpha G_I - \beta E_I + \chi P_I \quad (11)$$

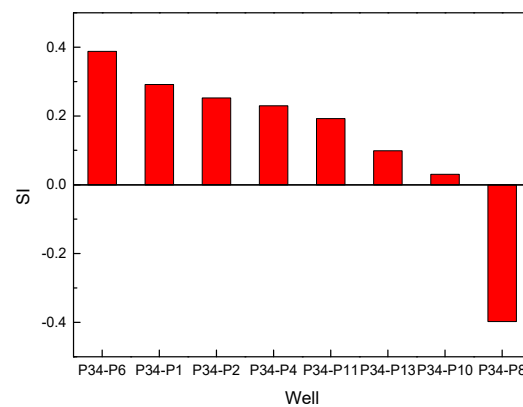
where  $\alpha$ ,  $\beta$ , and  $\gamma$  are the weight coefficients corresponding to each composite index.

## 5. Field Test and Results

There were 8 horizontal wells in the target test area, all of which have been put into operation for more than 2 years. The geological, completion, and production performance conditions of each horizontal well are similar. Refracturing technology is an important means to recover production capacity in the block at present. It is necessary to rank and evaluate the potential of refracturing candidate wells before formulating the refracturing construction scheme. Based on the established well selection method, the data of eight horizontal wells in the test area were collected and sorted, and the relevant evaluation indexes were calculated (Table 1). A range of standardization processing was carried out, and the relevant parameters were obtained as follows (Figure 10).

**Table 1.** Calculation result of decision index of horizontal well selection in the target test area.

Well	$G_I$	$E_I$	$P_I$	$S_I$
P34-P1	0.629	0.233	0.703	0.291
P34-P2	0.469	0.207	0.673	0.252
P34-P4	1.000	0.229	0.229	0.229
P34-P6	0.473	0.143	1.000	0.388
P34-P8	0.057	1.000	0.024	−0.398
P34-P10	0.058	0.363	0.510	0.030
P34-P11	0.380	0.190	0.538	0.192
P34-P13	0.395	0.186	0.237	0.099

**Figure 10.** Schematic diagram of well selection results.

As shown in the figure above, the stimulation potential of 8 horizontal wells in the X test area was ranked from large to small as P34-P6, P34-P1, P34-P2, P34-P4, P34-P11, P34-P13, P34-P10, and P34-P8. Therefore, in the development of a refracturing plan in the X test area, it was necessary to carry out refracturing for well P34-P6 and well P34-P1 first. Under the limitation of economic and technical conditions, the refracturing potential of P34-P8 and P34-P10 wells is small, so it was necessary to conduct an economic and technical evaluation to demonstrate the feasibility of refracturing.

Through the analysis of the basic situation of P34-P8 well, the length of the horizontal well and the drilling encounter rate of oil-bearing sandstone were small in the process of drilling and completion, and the fracturing fluid consumption was large in the initial fracturing process. In a word, the degree of primary fracturing in a unit horizontal well length was higher, so the feasibility of refracturing technology was not high, and the stimulation potential after refracturing was low. Therefore, it was not recommended to carry out refracturing technology.

By analyzing the target well P34-P6 of refracturing, the average effective thickness  $h_e$  was 2.3 m, the average porosity was 12.5 %, the average permeability  $K$  was 1.32 mD (The standard deviation was 1.0766), the footage  $L$  of the horizontal well was 840 m, the drilling rate of oil-bearing sandstone  $D_r$  was 84.9 %, the formation pressure  $P_i$  was 20.4 MPa, and the oil saturation  $S_o$  was 0.56. In the initial fracturing of well X-6, 9 clusters were fractured, the fracture spacing was 100 m, the initial fracturing fluid consumption was 14,400 m<sup>3</sup>, and the fracturing sand amount was 460 m<sup>3</sup>. After the initial fracturing, the average daily fluid level was 32 t, and the average daily oil production level was 10 t, and a good oil increase effect was achieved in the early stage of fracturing. With the increase in production time, the liquid production level gradually decreased. After 700 days of initial fracturing, the daily fluid level decreased to 3.8 t, and the daily oil level decreased to 1.9 t. The results of numerical simulation showed that the remaining oil between the fractures was rich, so the production of a single well can be increased by adding pressure between new fractures.

There were 18 fractures in the design and construction of refracturing. The overall construction was smooth, and sand was added to each fracturing section according to the design. After refracturing, micro seismic monitoring was carried out for a certain section of fracture (Figure 11). The green

response data point was the primary artificial fracture, and the red response data point was the refracturing artificial fracture. The monitoring results showed that the trend of the refracturing fracture was parallel to the primary fracture, and the new fracture was well spread between the old fracture, which effectively increased the oil drainage area of the reservoir. After refracturing, the whole reservoir was reformed more fully.

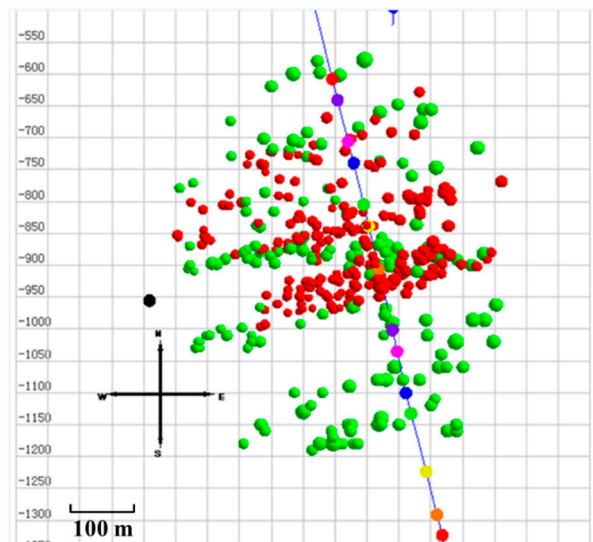


**Figure 11.** Micro seismic monitoring results after repeated fracturing.

The production performance of the well after refracturing was analyzed (Figure 12). At the initial stage after refracturing, the daily fluid production was 31 t, and the daily oil production was 10.2 t. Up to now, the well had been put into operation for 136 d after the refracturing measures, with an accumulative oil increase of 1150.7 t and a flow back rate of 82.1 %. The stimulation effect is obvious, which verifies the accuracy of the well selection results.

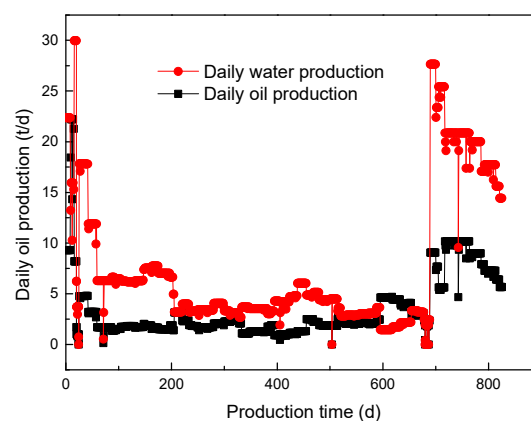


**Figure 12.** Target well production curve.

## 6. Conclusions

In this paper, from the perspective of geological engineering integration, a large number of numerical simulation models were designed, and the refracturing production database as constructed based on the actual field data set. The comprehensive index of geology, engineering, and production was constructed by the dimensionless parameter method, which has certain engineering or physical significance. The rationality of the comprehensive index was verified by analyzing the relationship between the comprehensive index and the refracturing oil production.

With the help of the deep learning method in the field of artificial intelligence, the XGBoost decision tree model was established. The comprehensive index of geology, engineering, and production was taken as the input term, and the incremental oil production by refracturing was taken as the output term. The correlation coefficient  $R^2$  between the actual value and the predicted value of the test set reached more than 0.9, which can be considered that the decision tree model established can reflect the reality. According to the actual situation, it was concluded that the weight of geological, engineering and production factors on the refracturing oil increment was 0.42, 0.33, and 0.25. It can be concluded that the fracturing completion in the initial fracturing stage had the highest impact on the refracturing effect, followed by the production and geological conditions after the initial fracturing.

Through the weighted average of the comprehensive index, the well selection decision index was constructed, which realized the fast well selection decision of multiple refracturing candidate wells in the target block, which is simple and fast. In view of an actual tight oil block, the established decision-making method of refracturing candidate wells was applied to optimize the target wells, and the refracturing test was carried out. The actual production data showed that the daily oil production after refracturing was restored to 10.18 t/d from 3.09 t/d. Therefore, it can be considered that the comprehensive decision-making index had good reliability.

The concept and unit of each symbol in the article (Table 2).

Table 2. Nomenclature.

Nomenclature	Concept	Units
$K$	Permeability	mD
$FCD$	Fracture conductivity	D-cm
$\Delta P$	Production pressure difference	MPa
$L$	Footage of horizontal well	m
$D_r$	Drilling rate of oil-bearing sandstone	%
$\Phi$	Porosity	%
$h_e$	Reservoir thickness	m
$V_s$	Fracturing fluid consumption	m <sup>3</sup>
$SP$	Fracturing sand–liquid ratio	%
$N$	Number of fracturing clusters	-
$P_i$	Reservoir pressure	MPa
$P_w$	Bottom hole flowing pressure	MPa
$N_l$	Cumulative liquid production	m <sup>3</sup>
$N_s$	Fracturing fluid flow back volume	m <sup>3</sup>
$C_{ob}$	Initial average yield	m <sup>3</sup> /d
$C_{oa}$	Overall average yield	m <sup>3</sup> /d
$N_o$	Cumulative oil production	m <sup>3</sup>
$\Delta Q$	Oil increase after refracturing	m <sup>3</sup>
$G_I$	Geological composite index	-
$E_I$	Engineering composite index	-
$P_I$	Production composite index	-
$S_I$	Comprehensive decision index	-

**Author Contributions:** Q.F. conceived and designed the experiments; Q.F., J.R., and X.Z. performed the experiments; Q.F., J.R., and S.W., analyzed the data; Q.F., X.W., and Y.L. wrote the paper. All authors have read and agreed to the published version of the manuscript.

**Funding:** This research was funded by the National Science and Technology Major Project (2017ZX05071).

**Conflicts of Interest:** The authors declare no conflict of interest.

## Appendix A

**Table A1.** Statistical table of geological parameters of tight oil wells in the target block.

Well Name	$P_i$	K	$\Phi$	$h_e$	$G_I$
X-1	19.1	1.54	0.146	3.2	0.27
X-2	21.2	1.37	0.125	4.1	0.43
X-3	21.6	1.32	0.125	2.7	0.16
X-4	20.26	0.56	0.127	5	0.15
X-5	18.4	2.31	0.163	2.5	0.16
X-6	20.8	1.32	0.125	4.7	0.04
X-7	22	1.37	0.125	2	0.24
X-8	18.2	1.5	0.118	4.4	0.53
X-9	18.2	2.31	0.163	2.4	0.36
X-10	18	1.23	0.139	4.4	0.46
X-11	22.1	0.37	0.125	4.5	0.15
X-12	19.2	1.54	0.146	4.5	0.67
X-13	20	1.32	0.125	3.4	0.20
X-14	20	1.32	0.125	4.7	0.04
X-15	19.5	1.8	0.163	5.3	1.00
X-16	20.2	1.32	0.125	7.1	0.42
X-17	17.9	1.5	0.118	4.4	0.48
X-18	21.6	1.32	0.125	2.7	0.16
X-19	20.4	1.32	0.125	4	0.20
X-20	17.8	1.5	0.118	4.4	0.55
X-21	18.5	1	0.132	4.6	0.26
X-22	20.4	1.32	0.125	5	0.26
X-23	18.2	1.8	0.163	3	0.11

**Table A2.** Statistical table of fracturing engineering parameters of tight oil wells in the target block.

Well Name	L	$D_r$	N	$V_s$	SP	$E_I$
X-1	1109	0.766	14	7616	0.1675	0.13
X-2	1384	1	39	19073	0.13	0.44
X-3	968	0.857	16	9669	0.159	0.19
X-4	1547	0.604	22	9461	0.1497	0.21
X-5	805	0.47	12	6906	0.308	0.42
X-6	491	0.246	5	9067	0.154	0.36
X-7	1669	0.96	16	16639	0.12	0.13
X-8	1580	0.968	20	6369	0.16	0.08
X-9	1136	0.798	16	7509	0.308	0.26
X-10	1505	0.904	19	11821	0.1371	0.14
X-11	1651	0.975	52	28600	0.129	0.75
X-12	1626	0.913	22	14000	0.159	0.21
X-13	1074	0.728	16	13013	0.1422	0.24
X-14	770	0.155	8	16983	0.14	1.00
X-15	1468	0.985	22	8600	0.155	0.13
X-16	958	0.833	16	12448	0.146	0.23
X-17	1438	0.973	13	17225	0.164	0.16
X-18	874	0.913	9	17029	0.158	0.19
X-19	880	0.761	12	8122.2	0.15656	0.14
X-20	1651	0.97	18	8872	0.207	0.13
X-21	990	0.971	21	10817	0.198	0.29
X-22	840	0.849	11	14399	0.1672	0.23
X-23	1027	0.274	17	8031	0.1513	0.46

**Table A3.** Statistical table of production parameters of tight oil wells in the target block.

Well Name	N <sub>s</sub>	N <sub>o</sub>	N <sub>l</sub>	C <sub>ob</sub>	C <sub>oa</sub>	P <sub>w</sub>	ΔQ	P <sub>I</sub>	S <sub>I</sub>
X-1	5026	1559	8160	1.99	1.40	9.6	4886	0.41	0.15
X-2	4840	5992	10811	7.71	4.18	4.87	4070	0.58	0.11
X-3	4804	6967	12559	9.00	4.64	10.1	2683	0.33	0.07
X-4	8050	16929	29773	20.50	8.97	4.8	1994	0.17	0.01
X-5	6735	7639	16722	10.40	7.20	6.7	6357	0.18	-0.08
X-6	4449	2787	6699	19.59	18.75	8.9	2792	0.58	0.05
X-7	5052	13135	20667	15.40	9.63	8.3	5643	0.14	0.05
X-8	5097	14804	21851	2.75	0.71	7.1	4978	0.03	0.11
X-9	4617	6129	12968	9.90	3.20	5	6262	0.62	0.19
X-10	7149	5027	14480	12.25	3.61	6.68	3548	0.95	0.37
X-11	4797	9591	13154	11.80	8.34	5	3515	0.27	-0.19
X-12	4567	5121	10237	9.97	6.74	4.8	3741	0.58	0.27
X-13	11353	4332	19831	7.32	6.02	5.7	4333	0.18	0.01
X-14	3618	4597	8594	16.37	13.30	10.6	2211	0.45	-0.26
X-15	3976	4377	9278	7.20	3.15	5.2	8402	0.90	0.49
X-16	4244	6098	11248	4.48	2.75	5.62	3227	0.21	0.08
X-17	3176	11410	16764	5.16	2.19	5.49	3449	0.09	0.08
X-18	2440	11399	16149	18.97	9.05	12	4466	0.22	0.03
X-19	6983	5996	15802	8.70	4.72	6.9	4191	0.37	0.11
X-20	5488	4352	10195	4.42	1.89	5.6	5357	0.54	0.26
X-21	6983	5996	15802	8.70	4.72	6.9	3986	0.31	0.05
X-22	2976	4377	9278	7.20	2.15	5.2	4658	1.00	0.30
X-23	5052	13135	20667	15.4	9.63	8.3	3703	0.10	-0.13

## References

- Zou, C.; Dong, D.; Wang, S.; Li, J.; Li, X.; Wang, Y.; Li, D.; Cheng, K. Geological characteristics and resource potential of shale gas in China. *Pet. Explor. Dev.* **2010**, *37*, 641–653. [[CrossRef](#)]
- Ren, G.; Jiang, J.; Younis, R.M. A Model for coupled geomechanics and multiphase flow in fractured porous media using embedded meshes. *Adv. Water Resour.* **2018**, *122*, 113–130. [[CrossRef](#)]
- Wang, T.; Wang, J. Catalytic Effect of Cobalt Additive on the Low Temperature Oxidation Characteristics of Changqing Tight Oil and Its SARA Fractions. *Energies* **2019**, *12*, 2848. [[CrossRef](#)]
- Nandlal, K.; Weijermars, R. Impact on Drained Rock Volume (DRV) of Storativity and Enhanced Permeability in Naturally Fractured Reservoirs: Upscaled Field Case from Hydraulic Fracturing Test Site (HFTS), Wolfcamp Formation, Midland Basin, West Texas. *Energies* **2019**, *12*, 3852. [[CrossRef](#)]
- Malpani, R.; Sinha, S.; Charry, L.; Sinosis, B.; Clark, B.; Gakhar, K. Improving Hydrocarbon Recovery of Horizontal Shale Wells Through Refracturing. Presented at the CSUR Unconventional Resources Conference, Calgary, AB, Canada, 20–22 October 2015.
- Urban, E.; Orozco, D.; Fragoso, A.; Selvan, K.; Aguilera, R. Refracturing Vs. Infill Drilling. A Cost Effective Approach to Enhancing Recovery in Shale Reservoirs. Presented at the Unconventional Resources Technology Conference, San Antonio, TX, USA, 1–3 August 2016.
- Indras, P.; Blankenship, C. A Commercial Evaluation of Refracturing Horizontal Shale Wells. Presented at the SPE Annual Technical Conference and Exhibition, Houston, TX, USA, 28–30 September 2015.
- Roussel, N.P.; Sharma, M.M. Selecting Candidate Wells for Refracturing Using Production Data. *Spe Prod. Oper.* **2013**, *28*, 36–45. [[CrossRef](#)]
- Sinha, S.; Ramakrishnan, H.A. Novel Screening Method for Selection of Horizontal Refracturing Candidates in Shale Gas Reservoirs. Presented at the North American Unconventional Gas Conference and Exhibition, The Woodlands, TX, USA, 14–16 June 2011.
- Tavassoli, S.; Yu, W.; Javadpour, F.; Sepehrnoori, K. Well screen and optimal time of refracturing: A Barnett shale well. *J. Pet. Eng.* **2013**, *36*, 12–22. [[CrossRef](#)]
- Oberwinkler, C.; Economides, J.M. The Definitive Identification of Candidate Wells for Refracturing. Presented at the SPE Annual Technical Conference and Exhibition, Denver, CO, USA, 5–8 October 2003.



12. Saeedi, A.; Camarda, V.K.; Liang, T.J. Using Neural Networks for Candidate Selection and Well Performance Prediction in Water-Shutoff Treatments Using Polymer Gels—A Field-Case Study. Presented at the SPE Asia Pacific Oil & Gas Conference and Exhibition, Adelaide, Australia, 11–13 September 2006.
13. Udegbe, E.; Morgan, E.; Srinivasan, S. Big-Data Analytics for Production-Data Classification Using Feature Detection: Application to Restimulation-Candidate Selection. *Soc. Pet. Eng.* **2019**, *22*, 364–385. [[CrossRef](#)]
14. Zeng, F.; Cheng, X.; Guo, J.; Tao, L.; Chen, Z. Hybridising Human Judgment, AHP, Grey Theory, and Fuzzy Expert Systems for Candidate Well Selection in Fractured Reservoirs. *Energies* **2017**, *10*, 447. [[CrossRef](#)]
15. Reeves, S.R.; Bastian, P.A.; Spivey, J.P.; Flumerfelt, R.W.; Mohaghegh, S.; Koperna, G.J. Benchmarking of Restimulation Candidate Selection Techniques in Layered, Tight Gas Sand Formations Using Reservoir Simulation. Presented at the SPE Annual Technical Conference and Exhibition, Dallas, TX, USA, 1–4 October 2000.
16. Reeves, S.R. Assessment of technology barriers and potential benefits of restimulation R and D for natural gas wells. Presented at the Final Report 1995-April 1996, Lake Tahoe, VA, USA, 1–3 October 1996.
17. Reese, L.J.; Britt, K.L.; Jones, R.J. Selecting Economic Refracturing Candidates. Presented at the SPE Annual Technical Conference and Exhibition, New Orleans, LA, USA, 25–28 September 1994.
18. Popa, S.A.; Mohaghegh, D.S.; Gaskari, R.; Ameri, S. Identification of Contaminated Data in Hydraulic Fracturing Databases: Application to the Codell Formation in the DJ Basin. Presented at the SPE Western Regional/AAPG Pacific Section Joint Meeting, Long Beach, CA, USA, 19–24 May 2003.
19. Zhou, Z.; Wei, S.; Lu, R.; Li, X. Numerical Study on the Effects of Imbibition on Gas Production and Shut-In Time Optimization in Woodford Shale Formation. *Energies* **2020**, *13*, 3222. [[CrossRef](#)]
20. Yu, W.; Sepehrnoori, K. Optimization of Well Spacing for Bakken Tight Oil Reservoirs. Presented at the Unconventional Resources Technology Conference, Denver, CO, USA, 25–27 August 2014.
21. Wantawin, M.; Yu, W.; Sepehrnoori, K. An Iterative Work Flow for History Matching by Use of Design of Experiment, Response-Surface Methodology, and Markov Chain Monte Carlo Algorithm Applied to Tight Oil Reservoirs. *Soc. Pet. Eng.* **2017**, *20*, 613–626. [[CrossRef](#)]
22. Nguyen, X.H.; Bae, W.; Gunadi, T.; Park, Y. Using response surface design for optimizing operating conditions in recovering heavy oil process, Peace River oil sands. *J. Pet. Sci. Eng.* **2014**, *117*, 37–45. [[CrossRef](#)]
23. Udy, J.; Hansen, B.; Maddux, S.; Petersen, D.; Heilner, S.; Stevens, K.; Lignell, D.; Hedengren, J.D. Review of field development optimization of waterflooding, eor, and well placement focusing on history matching and optimization algorithms. *Process* **2017**, *5*, 34.
24. Carpenter, C. Geology-Driven Estimated-Ultimate-Recovery Prediction with Deep Learning. *J. Pet. Technol.* **2016**, *68*, 74–75. [[CrossRef](#)]
25. Li, W. Classifying geological structure elements from seismic images using deep learning. *Seg. Tech. Program. Expand. Abstr.* **2018**. [[CrossRef](#)]
26. Pham, N.; Fomel, S.; Dunlap, D.B. Automatic channel detection using deep learning. *Interpretation* **2019**, *7*. [[CrossRef](#)]
27. Zha, W.; Li, X.; Xing, Y.; He, L.; Li, D. Reconstruction of shale image based on Wasserstein Generative Adversarial Networks with gradient penalty. *Adv. Geo Energy Res.* **2020**, *4*, 107–114. [[CrossRef](#)]
28. Sudakov, O.; Burnaev, E.; Koroteev, D. Driving digital rock towards machine learning: Predicting permeability with gradient boosting and deep neural networks. *Comput. Geosci.* **2019**, *127*, 91–98. [[CrossRef](#)]
29. Chen, T.; Guestrin, C. XGBoost: A Scalable Tree Boosting System. In Proceedings of the 22nd ACM SIGKDD International Conference on Knowledge Discovery and Data Mining, San Francisco, CA, USA, 13–17 August 2016.
30. Nguyen, H.; Bui, X.N.; Bui, H.B.; Cuong, D.T. Developing an XGBoost model to predict blast-induced peak particle velocity in an open-pit mine: A case study. *Acta Geophys.* **2019**, *67*, 477–490. [[CrossRef](#)]

